Analytical Biochemistry 612 (2021) 113957

Contents lists available at ScienceDirect

Analytical Biochemistry

journal homepage: www.elsevier.com/locate/yabio

Quantification of endospores in ancient permafrost using time-resolved terbium luminescence

S.J. Lalla [a], K.R. Kaneshige [a], D.R. Miller [a], R. Mackelprang [b], R. Mogul [a,*]

[a] Chemistry & Biochemistry Department, Cal Poly Pomona, Pomona, CA, 91768, USA
[b] Department of Biological Sciences, CSU Northridge, Northridge, CA, USA

ARTICLE INFO

Keywords:
Permafrost
Endospores
Abundance
Dipicolinic acid
Terbium
Luminescence

ABSTRACT

We describe herein a simple procedure for quantifying endospore abundances in ancient and organic-rich permafrost. We repeatedly (10x) extracted and fractionated permafrost using a tandem filter assembly composed of 3 and 0.2 μm filters. Then, the 0.2 μm filter was washed (7x), autoclaved, and the contents eluted, including dipicolinic acid (DPA). Time-resolved luminescence using Tb(EDTA) yielded a LOD of 1.46 nM DPA (6.55×10^3 endospores/mL). In review, DPA/endospore abundances were ~2.2-fold greater in older 33 ky permafrost (258 ± 36 pmol DPA gdw^{-1}; $1.15 \times 10^6 \pm 0.16 \times 10^6$ spores gdw^{-1}) versus younger 19 ky permafrost ($p = 0.007297$). This suggests that dormancy increases with permafrost age.

1. Technical note

Ancient permafrost (perennially frozen ground) persists for thousands of years, harboring a moderately diverse array of microbial life [1–3] along with large stores of organic carbon [4,5]. Climate change thaws permafrost [6,7] and presents a variety of potential environmental and health issues, including the release of greenhouse gases stemming from microbial degradation of organic carbon [8,9] and the revival of age-old microorganisms [10–12], inclusive of dormant endospores, such as those associated with anthrax outbreaks in the Arctic circle [10,13,14]. For homeland security and ecology purposes, therefore, the development of low-cost detection and quantification methods for endospores would greatly assist in expanding environmental sample analysis in developing nations and within the scientific community.

For permafrost, the few methods that describe endospore quantification are DNA-based and likely underestimate cell abundance due to DNA extraction inefficiencies [15]. Further, the substantial soil organic carbon (SOC) pool likely interferes with other non-DNA-based methods. In contrast, methods for non-permafrost soils and ice samples are well-described and include chemical, biochemical, and microbiological means such as luminescence spectroscopy [16–18], liquid chromatography [17,19], PCR [20,21], and cultivation [22,23]. Advantages to these collective methods include high sensitivities, roughly quantitative yields during extraction/separation [16,17], and phylogenetic identifications. However, challenges to these methodologies include high fluorescent backgrounds from SOC, lengthy extraction and preparation steps, complicated chromatographic methods, costs associated with soil DNA extraction kits and PCR reagents, slow cultivation times, and loss of abundance and diversity during cultivation.

In this report, therefore, we detail a simple procedure (Diagram 1) for quantifying bacterial endospore abundances in permafrost using a low-cost tandem filtration system followed by time-resolved lanthanide luminescence spectroscopy (Supplemental Methods). To address the challenges listed above, we used (A) relatively inexpensive reagents and materials, (B) time-saving and straightforward procedures, (C) a time-resolved luminescence approach to eliminate interferences from fluorescent SOC, and (D) a spectral procedure suitable for typical fluorescence spectrometers hosting a phosphorescence mode.

Bacterial endospores were quantitated using the biomarker 2,6-pyridinedicarboxylic acid, or dipicolinic acid, which serves roles in endospore stability and is predominantly (or only) found in endospores [24–26] at concentrations of ~0.2–1.2 M, as measured across strains from the genera of *Bacillus*, *Oceanobacillus*, *Desulfosporosinus*, *Desulfotomaculum*, and class of *Clostridiales* [16] (or 5–15% of the dry weight [27]). Dipicolinic acid (DPA) is aromatic, strongly absorbs in the UV, and forms tridentate metal chelates with lanthanides, such as terbium, to form complexes with differing stoichiometries $(Tb(DPA)_{1\text{-}3}(H_2O)_{0\text{-}6}$; assuming a 9-coordinate complex) [28–30]. Typical to many terbium complexes, $Tb(DPA)_n$ is luminescent, where excitation of DPA (at 270 nm) results in energy transfer to the terbium center, culminating with

* Corresponding author. Cal Poly Pomona, Chemistry & Biochemistry Department, 3801 W. Temple Ave., Pomona, CA, 91768, USA.
E-mail address: rmogul@cpp.edu (R. Mogul).

https://doi.org/10.1016/j.ab.2020.113957
Received 8 August 2020; Received in revised form 11 September 2020; Accepted 13 September 2020
Available online 19 September 2020
0003-2697/

signature emissions of visible light (Fig. 1A). The emissions are bright, long-lived (2.1 m s), and released in narrow bands (≤40 nm) with large Stokes shifts (220–355 nm); thus, collectively serving as excellent handles for analysis [16,28,31].

However, a drawback to endospore quantitation using $Tb(DPA)_{1\text{-}3}$ is that the luminescence is rather unstable (Fig. 1B), with ~25% of the initial brightness (*i.e.*, signal intensity) lost 100 s after mixing probe and extract [28]. This loss is due to competition from other metal-binding biochemical groups including glycosidic moieties, non-aromatic amino acids, and phospholipids, which can form non- or weakly luminescent complexes with terbium. Alternatively, we've shown that $[Tb(EDTA)]^{1-}$ is a superior probe to $[Tb(H_2O)_9]^{3+}$. As per Fig. 1A and B, complexes between Tb(EDTA) and DPA are brighter and more stable and, as a result, exhibit ~2-fold higher signal intensities (at 545 nm), and only a ~5% loss in signal when in extracts of *Bacillus* spores (after 100 s) [28].

Characterizations by luminescence spectroscopy suggest a stoichiometry of $Tb(EDTA)(DPA)_1$ for the target complex. In brief, comparisons of luminescent lifetimes across aqueous and D_2O solutions supported exclusion of water from the terbium coordination sphere (m = 0.34; Tb (EDTA) $(DPA)_n(H_2O)_m$); while the changes in lifetimes across a titration of increasing [DPA] supported binding of one DPA ligand. Titration experiments (Fig. 1C) were conducted using 10 μM Tb(EDTA) or Tb^{3+} and 0–150 μM DPA (in 0.1 NaOAc, pH 5.5). The changes in lifetimes across the titrations were then fitted to a modified version of the Hill equation ($\theta \approx \left(\Delta\tau/\Delta\tau_{max}\right) = [DPA]^n/([DPA]^n + (K_{50})^n)$). In this model, the sequential binding of multiple ligands was assumed to have a cooperative effect on the luminescence lifetime. For Tb^{3+}, sigmoidal changes in lifetime were obtained during formation of $Tb(DPA)_n$, and regressions provided $n = 2.79 \pm 0.06$, which was consistent with a complex stoichiometry of $Tb(DPA)_3$. In contrast, changes in lifetime for Tb(EDTA) were hyperbolic, with regressions providing $n = 1.39 \pm 0.03$, which correlated to a stoichiometry of $Tb(EDTA)(DPA)_1$. Accordingly, standard curves prepared using Tb(EDTA) and time-resolved conditions (delay = 0.1 m s, λ_{em} = 545 nm) assumed binding of 1 analyte per probe and provided a LOD of 1.46 nM DPA, which corresponded to 6.55×10^3 spores/mL, when considering an averaged abundance of 2.24×10^{-16} mol DPA per spore [16] (See Supplemental section & Table S1).

Endospore abundances were thus measured in Pleistocene-aged permafrost, which originally formed 19 and 33 ky before present. Samples were collected and analyzed as described [1,15], with microscopy and geochemistry showing decreased abundances of active microorganisms, yet increasing amounts of SOC in older permafrost (~900–1700 mg/L dissolved organic carbon, DOC). In context, these observations were suggestive of higher endospore abundances and background fluorescence in the older 33 ky samples. Therefore, to extract, separate, and quantitate endospores, our procedure relied upon fractionation of permafrost extracts based upon particle size, washing of captured endospores to remove the stores of SOC, release of DPA through autoclaving, and measurement of the luminescence in mixtures of Tb(EDTA) using a time-resolved approach.

As displayed in Fig. 2, use of temporal gating effectively eliminated interference from the SOC fluorescence; thereby, revealing a resolved terbium luminescence. As per control experiments, the Tb(EDTA) luminescence was sensitized (or increased) by SOC from extracts of non-autoclaved permafrost (@270 nm) (Fig. 2A) and quenched (or decreased) by SOC from extracts of autoclaved permafrost (Fig. 2B). In effect, these observations exemplified the necessity to minimize interferences from SOC, which was accomplished in this procedure by filtration, washing, and spectral selection. In addition, our results indicated that permafrost may be a novel source for natural product lanthanide sensitizers.

In the extractions, as detailed in the Supplemental Section, Fig. 3A, and **Diagram S1**, slightly-thawed permafrost (~0.5 g) was resuspended in 1.5 mL 0.10 M NaOAc (pH 5.5), mildly vortexed for 10 s, and allowed to gravity settle for ~1 min (for this study, buffer choice represented optimal conditions for downstream binding or chelation of DPA to the terbium probe). Upon settling of the suspension, the supernatant (~1 mL) was removed using a 1 mL plastic syringe, and fractionated through a tandem filter assembly composed of sequentially attached 3 and 0.2 μm syringe filters (Fig. S1A), with the eluate being saved for analysis. In this assembly, and as shown in Fig. S1B, larger soil particles (which provided substantial background fluorescence) were captured on the 3 μm filter (PVDF membrane); whereas endospores liberated through vortexing passed through the 3 μm filter and collected on the 0.2 μm filter (cellulose acetate membrane). In control experiments, 0.45 μm

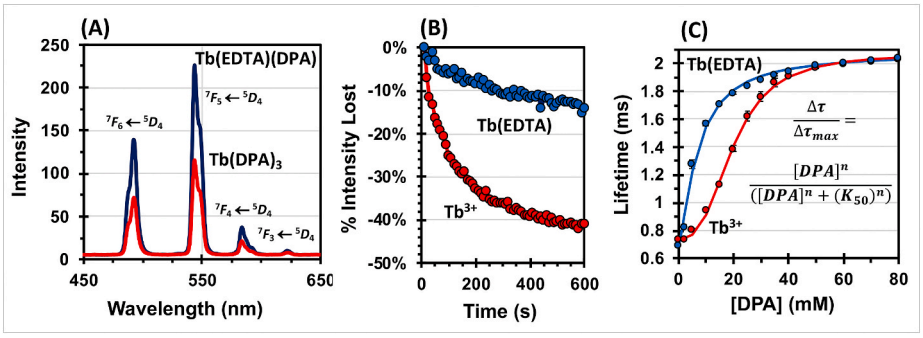

Fig. 1. Comparison of Tb(EDTA) and Tb^{3+}: (A) Luminescence emission spectra (λ_{ex} of 271 nm) for Tb(EDTA) (DPA) (blue) and $Tb(DPA)_3$ (red), where intensities are expressed as relative arbitrary units; (B) Luminescence stability in spore extracts, as obtained in kinetic studies (λ_{ex} = 271 nm, λ_{em} = 491 nm, 10 s intervals), where the percent loss in luminescence intensity (y-axis) was measured 10–600 s after mixing of Tb(EDTA) (blue) or Tb^{3+} (red) with extracts of *Bacillus* spores (in spore extracts, Tb (EDTA) loses a maximum of 28% of the initial intensity ($\%\Delta I_{max}$), while $Tb(H_2O)_9$ loses ~50%; for Tb(EDTA), the time required to lose half of the total change in intensity ($K_{0.5}$) is 570 s, while for Tb $(H_2O)_9$ half of the change in intensity is lost in 100 s; respective K_D values were 72 and 10^{-3}-10^{-6} μM for DPA binding to Tb(EDTA) and $Tb(H_2O)_9$), and respective luminescent brightness (k_L) values were 51 and 5.6 for Tb(EDTA)(DPA) and Tb(DPA) $(H2O)_6$), as adapted from Barnes et al., 2011; and (C) Profile of luminescent lifetimes across a titration of DPA for Tb(EDTA) (blue; circles) or Tb^{3+} (red; circles), where regressions (lines) were performed using an adapted version of the Hill equation, which provided values of $n = 1.39 \pm 0.03$ for Tb(EDTA) and $n = 2.79 \pm 0.06$ for Tb^{3+}, corresponding to Tb (EDTA) $(DPA)_1$ and $Tb(DPA)_3$. (For interpretation of the references to colour in this figure legend, the reader is referred to the Web version of this article.)

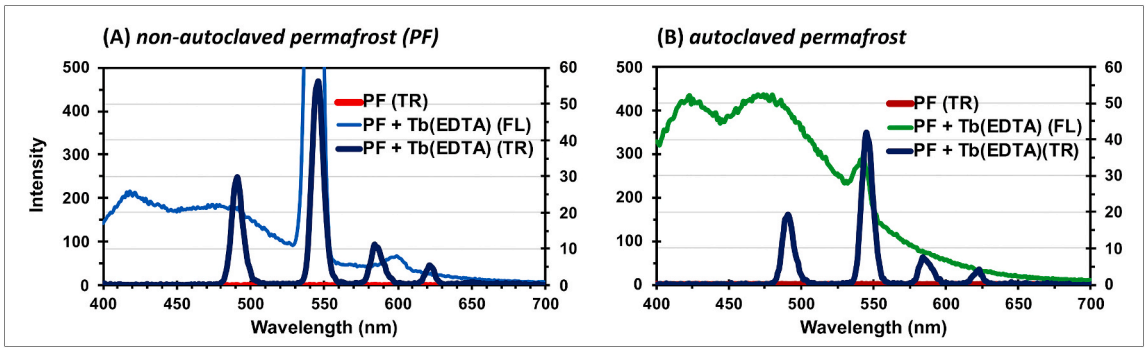

Fig. 2. Impacts of time-resolved (TR) measurements on the luminescence of Tb(EDTA) in extracts of (A) 19 ky permafrost and (B) autoclaved 19 ky permafrost, where spectra were obtained on a Cary Eclipse Fluorescence Spectrophotometer under fluorescence (FL; left y-axis) and phosphorescence modes (TR; right y-axis & gridlines), and intensities are expressed as relative arbitrary units; all samples (2.00 mL) contained 750 µL extract and 100 µM Tb(EDTA) in 0.100 M NaOAc (pH 5.5), and spectra were obtained using a λ_{ex} of 270 nm, emission window of 400–700 nm, 0.1 m s delay time, 5 nm excitation/emission band-pass, and 900 V PMT.

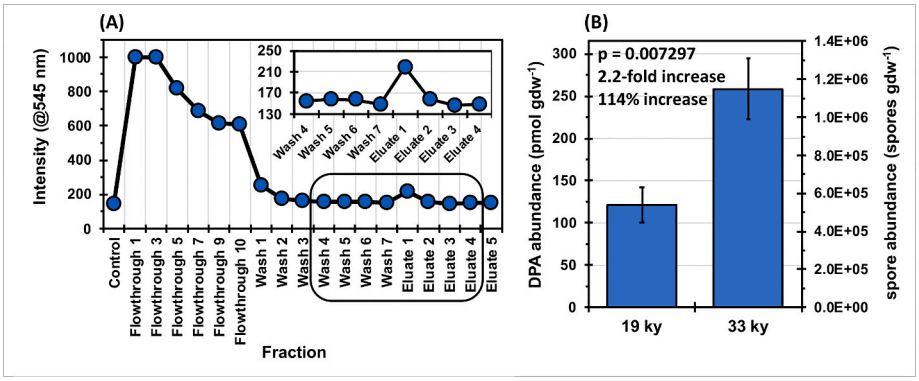

Fig. 3. Isolation and quantification of DPA and endospores: (A) Luminescence analysis of the tandem filtration procedure, where fractions obtained after tandem filtration (flowthrough), washes of the 0.2 µm filter (wash), and elutions of the autoclaved 0.2 µm filter (eluate) were mixed with Tb(EDTA) and the luminescence measured using a λ_{ex} = 270 nm, λ_{em} = 545 nm, and 0.1 m s delay time; inset plot represents the luminescence changes between Wash 4 and Eluate 4, (B) Abundances of DPA (left axis; pmol gdw^{-1}) and spores (right axis; spores gdw^{-1}) across the 19 and 33 ky permafrost samples; error bars represent the standard error (n = 8).

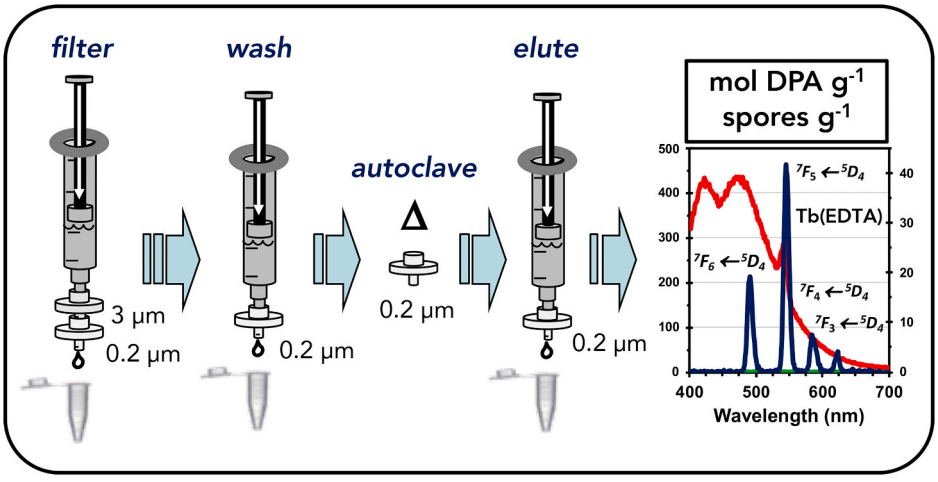

Diagram 1. Tandem filtration device and sequence of procedural steps including filtration of the extracts, washing of the 0.2 µm filter, autoclaving the 0.2 µm filter, elution of the contents, and spectral analysis of the sample.

filters showed poor retention of *Bacillus* endospores, while 5.0 µm filters provided insufficient removal of fluorescent SOC from the permafrost.

To maximize yield, the extraction/filtration procedure was repeated ten times (10x) using fresh aliquots of buffer, with all extracts being filtered through the same tandem assembly, and all eluates being retained as separate fractions for analytical measurements. The frequency of extraction/filtration steps was determined through control experiments with the 33 ky sample (Fig. S2A). In these experiments, eluate absorbances (~2–2.5) at 240 and 270 nm (within the linear range, Beckman DU640) decreased after each round of extraction/filtration, with a plateau occurring at ~0.3–0.4 after 10 successive steps – thereby indicating no further extraction of aqueous SOC (or DOC). Upon completion, the tandem filters were disconnected, the 3 µm filter removed, and the 0.2 µm filter washed seven times (7x) with buffer using a new plastic syringe. After the 7x washing steps, the 0.2 µm filter was autoclaved, and when cooled, attached to a plastic syringe, and the remaining bio/organic components eluted using five aliquots (5x) of buffer.

For luminescence spectroscopy [28], samples were 2.0 mL in total volume and prepared by mixing 750 μL of the eluate with a final concentration of 100 μM Tb(EDTA) in 0.100 M NaOAc (pH 5.5). Samples were manually mixed by continuous pipetting for ~30 s, and the luminescence measured on a Cary Eclipse Fluorescence Spectrophotometer in phosphorescence mode. Settings included a λ_{ex} of 270 nm, λ_{em} of 450–700 nm, delay time (or time resolution) of 0.1000 ms, 5.0 nm excitation/emission slit widths, and 900 V PMT voltage. Abundances of DPA were calculated using intensity values summed from the first two eluates, converted to [DPA] using the standard curve, translated to moles using the total eluate volume (typically ~1.5 mL), and expressed per gram dry weight of permafrost (moles DPA gdw^{-1}).

Results of the separation procedure are summarized in Fig. 3A (and further supported in the Supplemental section, Figs. S2A–D). Separations were monitored by following the change in luminescence across the collected fractions. Across the procedure, the plateau in absorbance and luminescence after the 10x extraction/filtration steps (flowthroughs 1–10) suggested that a majority of SOC had been extracted (Figs. S2A–B). Baseline luminescence values obtained after the 7x washes indicated substantial removal of SOC from the 0.2 μm filter (Fig. 3). Lastly, the increase in luminescence (eluates 1–2) after autoclaving (Fig. 3A inset plot) clearly indicated release of luminescent materials that (1) remained trapped on the filter during the 7x washing steps, (2) were soluble in the eluate buffer after autoclaving, and (3) functioned as a sensitizer for Tb(EDTA). As such, these results were consistent with the release of DPA by separation and isolation of spores using the tandem filter assembly.

As displayed in Fig. 3B, abundances of DPA increased from 121 ± 21 pmol DPA gdw^{-1} in 19 ky permafrost to 258 ± 36 pmol DPA gdw^{-1} in 33 ky permafrost (standard error, $n = 8$), as measured across 4 biological replicates from each age group, and 2 technical replicates per measure. These values translated to increases in endospore abundances from $5.38 \times 10^5 \pm 0.93 \times 10^5$ to $1.15 \times 10^6 \pm 0.16 \times 10^6$ spores gdw^{-1} (see Supplemental section). Thus, this corresponded to an ~2.2-fold (or 114%) increase in DPA/endospore abundances across the 19 and 33 ky permafrost samples ($p = 0.007297$, Student's *t*-test). These trends were supportive of dormancy serving increasing roles in survival across ancient permafrost.

For the tandem filtration assembly, yields of 52 ± 16% were obtained when using endospores of *Bacillus subtilis* ATCC 6633 (see Supplemental section). As such, for permafrost, correction of the endospore abundances (~1.0×10^6 & ~2.2×10^6 spores gdw^{-1}) amounted to ~4% and ~10% of the total stainable cells present in the 19 ky (2.8×10^7 cells gdw^{-1}) and 33 ky (2.3×10^7 cells gdw^{-1}) permafrost [15]. This corresponded to an ~2.5-fold increase in the percent of sporulated cells across the age groups, which further supported the assessment that older permafrost harbor increased endospore abundances. Critically, metagenomics studies [1] corroborate this assessment by showing ~1.5-fold increases in the abundances of genes associated with sporulation in older permafrost. Hence, both chemical measures and molecular genetics support dormancy as a survival mechanism in ancient permafrost.

In comparison to other measures, upper surface sediments (≤50 cm) of tidal flats (≤5.8×10^6 spores gdw^{-1}) [16] and bay waters (5.4×10^7 spores gdw^{-1}) [17] contain greater endospore biomasses than the perennially frozen 33 ky permafrost samples. However, these respective values represent ≤4% of the total cells, since these environments harbor higher relative cell abundances. These comparisons suggest that dormancy is a more dominant survival feature in ancient permafrost. In terms of methodology, the abundances for tidal flats and bay waters were obtained using the labile probe of $Tb(H_2O)_9$ with procedures requiring multi-step and multi-reagent extractions, or HPLC methods requiring ~4 h acid hydrolysis steps, ~1–3 h of additional sample processing, and considerable operational familiarity with liquid chromatography systems. In contrast, our method requires a total of 2–3 h per sample, utilizes low-cost reagents and supplies (*e.g.,* ~$22, 250 g, EDTA; ~$78, 5 g, $TbCl_3$; ~$166, 50, 0.2 μm filters; $83, 100, 3 μm filters), relies upon simple separation procedures, requires basic spectrometer functions, and is amenable to scientists from all disciplines. Therefore, our tandem filtration and time-resolved luminescence assay for spore quantification may serve as a reasonable, cost-effective, and time-saving tool for biodefense and microbial ecology applications.

Author contributions

All authors (SJL, KK, DRM, RMa, & RMo) contributed to acquisition/analysis of the data, critical reports/revisions of the work, approved the manuscript, and agreed to be accountable for the work. The primary investigator and corresponding author is RMo. RMa contributed to conception of the permafrost study; SJL performed probe preparation, spore characterizations, and permafrost analyses; KK measured luminescent lifetimes; and DRM prepared *Bacillus* spores.

Acknowledgments

This work was funded through the NASA Astrobiology Minority Institutional Research Support program (2016), and supported by the Chemistry and Biochemistry Department at Cal Poly Pomona, Pomona, CA. RMa acknowledges funding through the NASA Exobiology program #NNX15AM12G. We acknowledge contributions from Kelleen Chea regarding measurements of lifetimes, and Mark Waldrop and Thomas Douglas for vital roles in permafrost collection and associated biological and geochemical analysis.

Appendix A. Supplementary data

Supplementary data to this article can be found online at https://doi.org/10.1016/j.ab.2020.113957.

References

[1] R. Mackelprang, A. Burkert, M. Haw, T. Mahendrarajah, C.H. Conaway, T. A. Douglas, M.P. Waldrop, Microbial survival strategies in ancient permafrost: insights from metagenomics, ISME J. 11 (2017) 2305–2318.
[2] P. Singh, S.M. Singh, R.N. Singh, S. Naik, U. Roy, A. Srivastava, M. Bölter, Bacterial communities in ancient permafrost profiles of Svalbard, Arctic, J. Basic Microbiol. 57 (2017) 1018–1036.
[3] T.A. Vishnivetskaya, M.A. Petrova, J. Urbance, M. Ponder, C.L. Moyer, D. A. Gilichinsky, J.M. Tiedje, Bacterial community in ancient Siberian permafrost as characterized by culture and culture-independent methods, Astrobiology 6 (2006) 400–414.
[4] S. Schaphoff, U. Heyder, S. Ostberg, D. Gerten, J. Heinke, W. Lucht, Contribution of permafrost soils to the global carbon budget, Environ. Res. Lett. 8 (2013), 014026.
[5] C. Tarnocai, J. Canadell, E.A. Schuur, P. Kuhry, G. Mazhitova, S. Zimov, Soil organic carbon pools in the northern circumpolar permafrost region, Global Biogeochem. Cycles 23 (2009).
[6] C. Plaza, E. Pegoraro, R. Bracho, G. Celis, K.G. Crummer, J.A. Hutchings, C.E. H. Pries, M. Mauritz, S.M. Natali, V.G. Salmon, Direct observation of permafrost degradation and rapid soil carbon loss in tundra, Nat. Geosci. 12 (2019) 627–631.
[7] C.D. Koven, D.M. Lawrence, W.J. Riley, Permafrost carbon– climate feedback is sensitive to deep soil carbon decomposability but not deep soil nitrogen dynamics, Proc. Natl. Acad. Sci. Unit. States Am. 112 (2015) 3752–3757.
[8] C. Knoblauch, C. Beer, S. Liebner, M.N. Grigoriev, E.-M. Pfeiffer, Methane production as key to the greenhouse gas budget of thawing permafrost, Nat. Clim. Change 8 (2018) 309–312.
[9] E.A. Schuur, A.D. McGuire, C. Schädel, G. Grosse, J. Harden, D.J. Hayes, G. Hugelius, C.D. Koven, P. Kuhry, D.M. Lawrence, Climate change and the permafrost carbon feedback, Nature 520 (2015) 171–179.
[10] V. Timofeev, I. Bahtejeva, R. Mironova, G. Titareva, I. Lev, D. Christiany, A. Borzilov, A. Bogun, G. Vergnaud, Insights from *Bacillus anthracis* strains isolated from permafrost in the tundra zone of Russia, PLoS One 14 (2019), e0209140.
[11] T. Vishnivetskaya, S. Kathariou, J. McGrath, D. Gilichinsky, J.M. Tiedje, Low-temperature recovery strategies for the isolation of bacteria from ancient permafrost sediments, Extremophiles 4 (2000) 165–173.
[12] E.V. Pikuta, D. Marsic, A. Bej, J. Tang, P. Krader, R.B. Hoover, *Carnobacterium pleistocenium* sp. nov., a novel psychrotolerant, facultative anaerobe isolated from permafrost of the Fox Tunnel in Alaska, Int. J. Syst. Evol. Microbiol. 55 (2005) 473–478.
[13] K. Hueffer, D. Drown, V. Romanovsky, T. Hennessy, Factors Contributing to Anthrax Outbreaks in the Circumpolar North, EcoHealth, 2020, pp. 1–7.
[14] M.G. Walsh, A.W. de Smalen, S.M. Mor, Climatic influence on anthrax suitability in warming northern latitudes, Sci. Rep. 8 (2018) 9269.

[15] A. Burkert, T.A. Douglas, M.P. Waldrop, R. Mackelprang, Changes in the active, dead, and dormant microbial community structure across a Pleistocene permafrost chronosequence, Appl. Environ. Microbiol. 85 (2019).
[16] J. Fichtel, J. Köster, J. Rullkötter, H. Sass, Spore dipicolinic acid contents used for estimating the number of endospores in sediments, FEMS Microbiol. Ecol. 61 (2007) 522–532.
[17] B.A. Lomstein, B.B. Jørgensen, Pre-column liquid chromatographic determination of dipicolinic acid from bacterial endospores, Limnol Oceanogr. Methods 10 (2012) 227–233.
[18] H.S. Shafaat, A. Ponce, Applications of a rapid endospore viability assay for monitoring UV inactivation and characterizing arctic ice cores, Appl. Environ. Microbiol. 72 (2006) 6808–6814.
[19] J. Fichtel, J. Köster, B. Scholz-Böttcher, H. Sass, J. Rullkötter, A highly sensitive HPLC method for determination of nanomolar concentrations of dipicolinic acid, a characteristic constituent of bacterial endospores, J. Microbiol. Methods 70 (2007) 319–327.
[20] V. Sedlackova, R. Dziedzinska, V. Babak, P. Kralik, The detection and quantification of *Bacillus thuringiensis* spores from soil and swabs using quantitative PCR as a model system for routine diagnostics of *Bacillus anthracis*, J. Appl. Microbiol. 123 (2017) 116–123.
[21] C. Ryu, K. Lee, C. Yoo, W.K. Seong, H.B. Oh, Sensitive and rapid quantitative detection of anthrax spores isolated from soil samples by real-time PCR, Microbiol. Immunol. 47 (2003) 693–699.
[22] W.L. Nicholson, J.F. Law, Method for purification of bacterial endospores from soils: UV resistance of natural Sonoran desert soil populations of *Bacillus* spp. with reference to *B. subtilis* strain 168, J. Microbiol. Methods 35 (1999) 13–21.
[23] J. Gerdemann, T. Nicolson, Endogone spores in cultivated soils, Nature 195 (1962) 308–309.
[24] A. Aronson, P. Fitz-James, Structure and morphogenesis of the bacterial spore coat, Bacteriol. Rev. 40 (1976) 360.
[25] P. Setlow, I will survive: DNA protection in bacterial spores, Trends Microbiol. 15 (2007) 172–180.
[26] M. Paidhungat, B. Setlow, A. Driks, P. Setlow, Characterization of spores of *Bacillus subtilis* which lack dipicolinic acid, J. Bacteriol. 182 (2000) 5505–5512.
[27] W. Murrell, Chemical composition of spores and spore structures, in: G. Gould, A. Hurst (Eds.), The Bacterial Spore, 1, Academic Press, London, 1969.
[28] L. Barnes, K. Kaneshige, J. Strong, K. Tan, H. von Bremen, R. Mogul, Effects of terbium chelate structure on dipicolinate ligation and the detection of *Bacillus* spores, J. Inorg. Biochem. 105 (2011) 1580–1588.
[29] G. Jones, V.I. Vullev, Medium effects on the stability of terbium(III) complexes with pyridine-2,6-dicarboxylate, J. Phys. Chem. 106 (2002) 8213–8222.
[30] G. Jones, V.I. Vullev, Medium effects on the photophysical properties of terbium (III) complexes with pyridine-2,6-dicarboxylate, Photochem. Photobiol. Sci. 1 (2002) 925–933.
[31] A. Hagan, T. Zuchner, Lanthanide-based time-resolved luminescence immunoassays, Anal. Bioanal. Chem. 400 (2011) 2847–2864.